Author(s): Nonappa, Johannes S. Haataja, Jaakko V. I. Timonen, Sami Malola, Peter Engelhardt, Nikolay Houbenov, Manu Lahtinen, Hannu Häkkinen, and Olli Ikkala

Title: Reversible Supracolloidal Self-Assembly of Cobalt Nanoparticles to Hollow Capsids and Their Superstructures

Year: 2017

Version: Final published version

Please cite the original version:

Nonappa, Johannes S. Haataja, Jaakko V. I. Timonen, Sami Malola, Peter Engelhardt, Nikolay Houbenov, Manu Lahtinen, Hannu Häkkinen, and Olli Ikkala. Reversible Supracolloidal Self-Assembly of Cobalt Nanoparticles to Hollow Capsids and Their Superstructures . Angew. Chem. Int. Ed., 56, 6473-6477, May 2017. DOI: 10.1002/anie.201701135.

Colloidal Self-Assembly

International Edition: DOI: 10.1002/anie.201701135
German Edition: DOI: 10.1002/ange.201701135

Reversible Supracolloidal Self-Assembly of Cobalt Nanoparticles to Hollow Capsids and Their Superstructures

Nonappa, Johannes S. Haataja, Jaakko V. I. Timonen, Sami Malola, Peter Engelhardt, Nikolay Houbenov, Manu Lahtinen, Hannu Häkkinen,* and Olli Ikkala**

Abstract: *The synthesis and spontaneous, reversible supracolloidal hydrogen bond-driven self-assembly of cobalt nanoparticles (CoNPs) into hollow shell-like capsids and their directed assembly to higher order superstructures is presented. CoNPs and capsids form in one step upon mixing dicobalt octacarbonyl (Co_2CO_8) and p-aminobenzoic acid (pABA) in 1,2-dichlorobenzene using heating-up synthesis without additional catalysts or stabilizers. This leads to pABA capped CoNPs (core ca. 5 nm) with a narrow size distribution. They spontaneously assemble into tunable spherical capsids ($d \approx 50$–200 nm) with a few-layered shells, as driven by inter-nanoparticle hydrogen bonds thus warranting supracolloidal self-assembly. The capsids can be reversibly disassembled and reassembled by controlling the hydrogen bonds upon heating or solvent exchanges. The superparamagnetic nature of CoNPs allows magnetic-field-directed self-assembly of capsids to capsid chains due to an interplay of induced dipoles and inter-capsid hydrogen bonds. Finally, self-assembly on air–water interface furnishes lightweight colloidal framework films.*

In materials science, there is a growing need towards ever more advanced and hierarchical assemblies of colloids and nanoparticles.[1] Colloidal self-assembly is more difficult to master than the molecular self-assembly owing to challenges in controlling polydispersity, directionality, and aggregation.[2] Still, several types of colloidal self-assemblies have been recently demonstrated using inorganic and organic structural units.[1–20] More specifically, related to colloidal self-assembly towards hollow structures, viral capsids provide inspiration via the hydrogen bond-driven reversible self-assembly of shape-matching proteinic units.[21] In synthetic chemistry, hollow spherical superstructures using colloids have been achieved using sacrificial templates, atomic layer deposition, and selective oxidation.[22] However, they typically involve templating, several steps, and purifications, and do not allow spontaneous and reversible disassembly and re-assembly of hollow capsid-like superstructures. Recently, water-dispersible polydispersed CdS nanoparticles showed stabilizer-free spontaneous assembly into porous nanoshell-like structures.[23] The mechanism was attributed to electrostatic interactions, dispersion, and other colloidal forces and was supported by molecular dynamics simulations.

We recently reported template-free supracolloidal hydrogen-bonded self-assembly of water-dispersible gold nanoclusters to 2D nanosheets and spherical capsids with monolayer-thick shells by tuning the solvent conditions, given that the nanoclusters were atomically precise.[20] The self-assembly was driven by the ligands via carboxylic acid hydrogen bonding dimerization between the neighbouring nanoparticles. Such a self-assembly was attributed to the slightly non-spherical nature of the nanoparticles and the preferential alignment of hydrogen-bonding ligands into the nanoparticle equatorial plane. However, the synthesis of atomically precise nanoclusters is laborious, and it becomes relevant to ask whether synthetic reversible capsids can be achieved by a simple and scalable synthesis.

Cobalt nanoparticles are a relevant model system to study nanoscale magnetic properties.[24a] A typical synthesis involves the hot-injection or heating-up method using dicobalt octacarbonyl $Co_2(CO)_8$ and surfactants (for example, oleic acid or oleyl amine) in the presence of trioctyl phosphine oxide (TOPO).[24] The surfactants promote the dispersion and reduce aggregation in organic solvents, whereas TOPO catalyzes the decomposition of $Co_2(CO)_8$.

Herein, we report a facile synthesis of superparamagnetic cobalt nanoparticles (CoNPs), their in situ template-free reversible self-assembly to magnetic capsids driven by hydrogen bonds between the ligands, and their higher order superstructures by directed self-assembly. We envisaged ditopic ligands where one end selectively binds to CoNPs and simultaneously stabilizes them, whereas the other end makes hydrogen bonds between the CoNPs. Furthermore, we avoid additional catalysts/stabilizers as they might disturb the supramolecular interactions. We choose ditopic ligands containing amine ($-NH_2$) and carboxylic acid ($-COOH$) ends, as separated by a linker. Whereas the amine binds to the metal

[*] Dr. Nonappa, J. S. Haataja, Prof. J. V. I. Timonen, Dr. P. Engelhardt, Dr. N. Houbenov, Prof. O. Ikkala
Department of Applied Physics, Aalto University School of Science
Puumiehenkuja 2, 02150 Espoo (Finland)
E-mail: nonappa@aalto.fi
olli.ikkala@aalto.fi
Dr. S. Malola, Prof. H. Häkkinen
Departments of Chemistry and Physics, Nanoscience centre
University of Jyväskylä
Survontie 9, 40014 Jyväskylä (Finland)
E-mail: hannu.j.hakkinen@jyu.fi
Dr. P. Engelhardt
Department of Pathology and Virology, Haartman Institute
University of Helsinki
P.O. Box 21, 00014 Helsinki (Finland)
Dr. M. Lahtinen
Department of Chemistry, University of Jyväskylä
Survontie 9, 40014 Jyväskylä (Finland)
Supporting information and the ORCID identification number(s) for the author(s) of this article can be found under: https://doi.org/10.1002/anie.201701135.

surface and stabilizes the nanoparticles, the carboxylic acid group allows inter-nanoparticle hydrogen bonding.

Our prototypical synthesis involves heating a mixture of $Co_2(CO)_8$ and *p*-aminobenzoic acid (*p*ABA) in 1.0 mol/0.4 mol ratio in 1,2-dichlorobenzene (1,2-DCB) from room temperature to 165 °C and holding at this temperature for 30 min (Figure 1 a, see the Supporting Information and Figure S1 therein). The approach allows synthesis of CoNPs ($d \approx 5$ nm) with *p*ABA ligands and their spontaneous in situ, template-free self-assembly to larger spherical superstructures with sizes of about 200 nm after cooling to room temperature (Figure 1 b–e; cryo-TEM and dynamic light scattering in the Supporting Information, Figure S2). Electron tomographic reconstruction (ET) shows that the spherical superstructures possess circa 25–30 nm thick shells of densely packed CoNPs (Figure 1 f; Supporting Information, Videos S1–S3), and there is no packing order within the shells (Supporting Information, Figure S3). Such shell-like nanoparticle assemblies are here denoted as capsids. The individual nanoparticle sizes can be tuned from 5 nm to 10 nm by decreasing the mole fraction of *p*ABA vs. $Co_2(CO)_8$ from 0.4 to 0.06. At the same time, the average capsid diameter is decreased from circa 200 nm to 80 nm (Figure 1 g; Supporting Information, Figure S4). The contrast difference between the shells and interiors varies among the capsids (Figure 1 b–d). However, 3D reconstructions revealed that the shell thickness of the capsids remains similar (ca. 25 nm; Supporting Information, Figure S3). The contrast difference is attributed to different levels of kinetically trapped *p*ABA ligands, which are not bound to cobalt. The capsids without trapped *p*ABA show a clear difference between the shell (dark) and interior (gray) in their 2D projection (Figure 1 c). On the other hand, capsids with more trapped *p*ABAs show less contrast difference in their 2D projection (Figure 1 d).

The excess unbound *p*ABA molecules can be removed by soaking the capsids in acetone (Figure 2 a–c; Supporting Information, Figures S5, S6), as *p*ABA is soluble in acetone, and the trapped *p*ABAs are transported through the porous shell in analogy to processes in colloidosomes,[25] as revealed by ET reconstruction (Figure 2 c; Supporting Information, Videos S4, S5). That the capsid interior can contain trapped unbound *p*ABAs is also suggested by the ^1H and ^{13}C NMR spectroscopy (Supporting Information, Figure S7) and can be controlled by processing kinetics (Supporting Information, Figure S8).

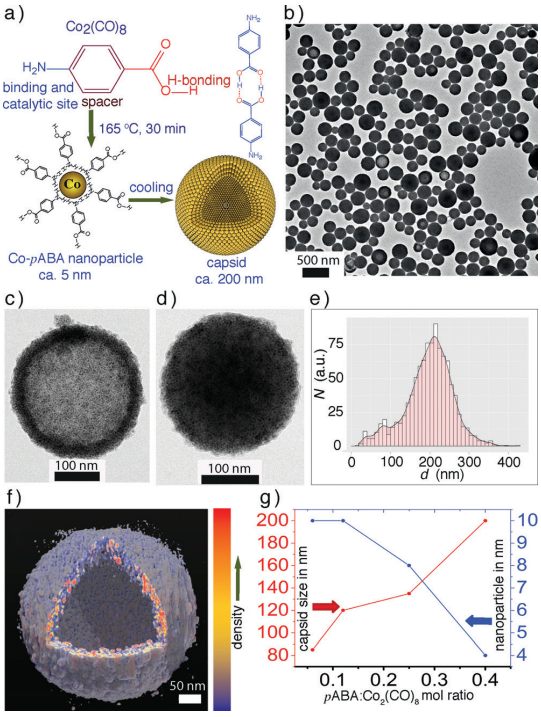

Figure 1. The overall concept. a) Heating-up synthesis of of CoNPs using $Co_2(CO)_8$ and *p*ABA in 1,2-DCB and their spontaneous self-assembly to shell-like capsids. b) TEM images showing spherical capsids for $Co_2(CO)_8$/*p*ABA 1.0/0.4 mol/mol. Capsids with less (c) and more (d) of kinetically trapped *p*ABA in the interior. e) Size distribution of capsids. f) ET reconstruction resolves clearly the CoNP shell layer from the hollow interior (see the Supporting Information, Figure S3 for a capsid with trapped *p*ABA in the interior). g) The nanoparticle and capsid sizes are tunable by the composition.

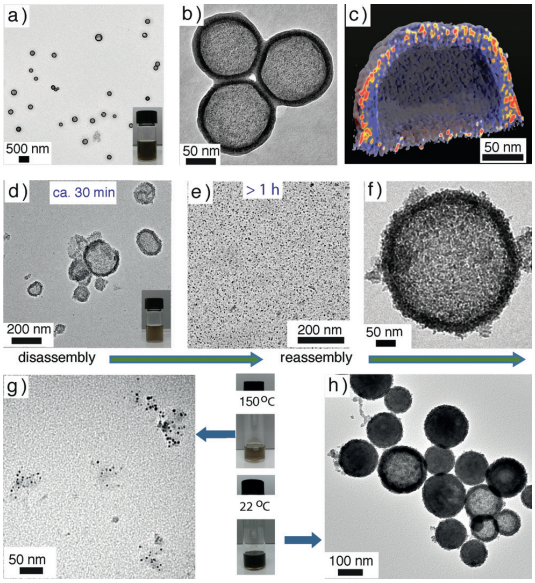

Figure 2. Thermal and solvent-exchange-driven reversibility of the capsids. a) TEM images of capsids after dispersing in acetone, the trapped *p*ABA ligands are removed. b) Interacting capsids in acetone as mediated by intercapsid hydrogen bonding. c) ET reconstruction of an acetone treated capsid. TEM images showing the disassembly of the capsids upon dispersing in methanol for d) 30 min and e) > 1 h. f) The methanol-treated CoNPs reassemble upon transferring to 1,2-DCB. g) The capsids dis-assemble upon heating and reassemble upon cooling (h).

We will next show that carboxylic acid hydrogen bonding between the ligands of the neighbouring Co-*p*ABA nanoparticles is important for the capsid formation. A direct evidence for existence of hydrogen bonds is obtained by FTIR spectroscopy (Supporting Information, Figure S9) and supported by solvent and thermal induced reversibility. The capsids disassemble into individual nanoparticles ($d \approx 5$ nm) in methanol (Figure 2d,e; Supporting Information, Figure S10) owing to the disruption of inter-nanoparticle hydrogen bonds. After dispersing the capsids in methanol, the excess *p*ABAs were removed by repeated washing and centrifugation. This allows colloidal dispersion without any unbound *p*ABA. When the purified CoNPs were redispersed in 1,2-DCB, they re-assembled into hollow spherical capsids (Figures 2f; Supporting Information, Figure S10), suggesting that the self-assembly is template-free. Further, when a solution of *p*ABA in 1,2-DCB was added to the purified dispersion of CoNPs, they reassembled into hollow capsids. However, the presence of *p*ABA resulted in capsid chains. Secondly, heating of Co-*p*ABA capsids in 1,2-DCB to about 150 °C resulted in disassembly to individual nanoparticles and reassembly upon cooling to room temperature (Figure 2g,h).

This is expected, as in pure benzoic acid the hydrogen bonding dimerization constant is reduced to about 4% from the room temperature value upon heating to 150 °C in a medium with a dielectric constant of 9.93, corresponding to 1,2-DCB (Supporting Information, Figures S11, S12).[26]

Note that the reversible self-assembly of the CoNPs to spherical capsids with a few-layer-thick shell takes place without any amphiphilicity of the building units, that is, unlike vesicles, dendrosomes, and polymersomes that have a molecular conformation that is adjustable upon packing.[27] In our system we deal with the hydrogen bond driven packing of structurally rigid colloidal level building blocks (metal nanoparticles; Supporting Information, Figure S3) to spherical superstructures. We denote these assemblies as capsids, as inspired by the viral capsids, that are formed by the H-bonding self-assembly of proteinic subunits.

To emphasize the novelty, we next describe ligands that do not allow capsids (see Figure 3a). First, random aggregates instead of capsids are obtained when heating-up synthesis was performed with only $Co_2(CO)_8$, suggesting the importance of ligands. Similarly, no capsids were formed with a mixture of $Co_2(CO)_8$/TOPO; where the single functional group binds on metal core, and the peripheral moiety is nonfunctional. Importantly, heating up synthesis of a mixture of $Co_2(CO)_8$, TOPO, and *p*ABA also furnished random aggregates (Supporting Information, Figure S13), indicating that the presence of additional stabilizers interferes with nanoparticle formation and self-assembly. Unlike *p*ABA, the *ortho*-ABA and *meta*-ABA did not lead to the capsids, where the steric hindrance of carboxylic groups limits the interparticle hydrogen bonding (Supporting Information, Figure S14). Capsids were neither observed if the peripheral group of the ligand forms only weak hydrogen bonds, such as the hydroxy–hydroxy hydrogen bond between two aminophenols. These findings suggest that the key to capsid formation is in the ditopic structure of the ligands, which contain a metal binding amino group and a hydrogen bonding peripheral carboxylic acid motif with a linker.

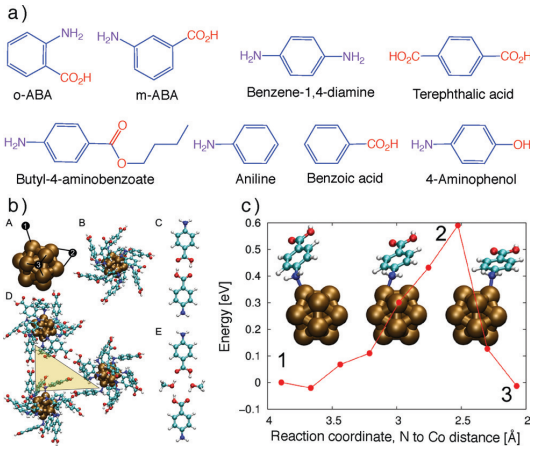

Figure 3. Understanding the ligands. a) Ligands that do not render capsids. b) Computational modeling: A) Co_{13} model cluster; B) Co_{13}*p*ABA_{12} model structure showing amines binding to nanoparticle surface leaving −COOH for inter-particle H-bonding; C) H-bonded *p*ABA dimer; D) Trimeric superstructure showing a triangular pore due to packing frustration; E) H-bonding in the *p*ABA-methanol complex. c) Diffusion barrier for a *p*ABA movement between two Co-top sites in the Co_{13}*p*ABA_{12} cluster calculated by using constrained relaxation. The reaction coordinate is defined as the distance between the N atom of *p*ABA and the Co atom where it is bound at configuration no. 3.

The role of hydrogen bonding in capsid formation, binding energy, diffusion barrier for ligand rearrangements, and magnetic moments of a model spherical cluster Co_{13}-*p*ABA_{12} was studied using density functional theory (DFT). We used spin-polarized density-functional theory with projector augmented waves (PAW) as implemented in the real-space grid code-package GPAW,[28] to study the ground state electronic structure and binding of *p*ABA ligands to model Co_{13} clusters (Figure 3b, see the Supporting Information for details).

Optimized structures of the model clusters and molecules are shown in Figure 3b. Bare cobalt cluster Co_{13} and the core of the fully protected cluster Co_{13}*p*ABA_{12} are of the same symmetry. The average binding energy of one *p*ABA molecule in the Co_{13}*p*ABA_{12} cluster is 0.62 eV (Supporting Information, Table S1). It is interesting to note that the calculated diffusion barrier for one *p*ABA molecule on top of the Co_{13} cluster is of the same order (ca. 0.6 eV, see Figure 3c). This suggests facile ligand rearrangement around nanoparticle surface. The ligand-protected Co_{13} cluster has a relatively large magnetic moment of 1.6 Bohr magneton per atom.

We also looked at the interaction between the *p*ABA dimers and the modification of the interaction by methanol (Figure 3b, parts C,E). The *p*ABA dimer is bonded by 0.39 eV per hydrogen bond. The bonding becomes slightly weaker (0.35 eV per hydrogen bond) in the presence of methanol. This indicates the possibility that methanol disturbs the capsid formation, as also observed experimentally.

Because of the curvature of the ligand surface, each $Co_{13}pABA_{12}$ cluster can make just a few hydrogen bonds to neighbouring clusters, leaving pores between the clusters (see Figure 3b, part D).

To explain in detail the thin shell formation, the exact ligand arrangement around the nanoparticles should be known. Owing to the polydispersity, single crystals cannot be grown, unlike in the atomically precise Au nanoparticles.[29] Still, we expect that, similarly, in the present case there exists a nonspherical arrangement of the ligands, leading to sheets that close towards shells. We trapped the intermediates of self-assembly by rapid cooling of reaction mixture in liquid nitrogen, which shows individual nanoparticles and partially assembled sheet-like structures (Supporting Information, Figure S16). Furthermore, the reaction was monitored at different time intervals using TEM, which revealed the intermediate structures (Supporting Information, Figure S17). The electron tomography, X-ray powder diffraction, thermoanalytical studies, and HR-TEM of capsids further supports the lack of packing order with overall amorphous nature of capsids (Supporting Information, Figures S18, S19).

Next, higher-level structures based on capsids were pursued by directed self-assembly. We showed above that the carboxylic acid mediated hydrogen bonds stabilize the capsids. Moreover, Figure 2b showed that inter-capsid hydrogen bonding can be achieved but without directionality. It is well-known that magnetic forces induce the formation of pearl/necklace-like 1D chains of magnetic nanoparticles.[10] The Co-*p*ABA capsids are superparamagnetic owing to their small size of constituent nanoparticles (experimentally determined magnetic core diameter ca. 3.2 nm, Figure 4a; see the Supporting Information for details). First, even application of a very high magnetic field of 9.4 T did not lead to disassembly of the capsids. Instead, directed self-assembly of capsids to 1D chains by induced dipoles of the capsids was observed even using low external magnetic field at 0.65 T (Figure 4b). A subtlety is involved, as after removing the magnetic field, the 1D chain of spherical capsids remained intact, due to inter-capsid hydrogen bondings facilitated by an ensemble of Co-*p*ABA nanoparticles at the two dipoles, as can be shown using TEM, SEM, AFM, and ET reconstruction at zero magnetic field (Figure 4c; Supporting Information, Movies S6, S7 and Figures S20–S22). The role of the stabilizing hydrogen bonds between the capsids can be further revealed by solvent exchanges. Even if the chains are robust in solvents, which do not disturb the hydrogen bonds (like 1,2-DCB), exposing the capsid chains to acetone leads to slow dis-assembly of the chains with time, due to the gradual opening of the intercapsid hydrogen bonds (Figure 4d). Note that previously the chains of individual nanoparticles have been stable only in the presence of magnetic field and they collapse upon removal of the magnetic field.[11] Our approach can be understood by magnetic field assisted manipulation of the colloidal objects into 1D colloidal chains to drive hydrogen bonding gluing to stabilize the capsid chains.

Finally, we extend the processing-directed supramolecular gluing between the capsids towards 3D bulk porous metallic nanoparticle network materials. We used interfacial self-assembly by placing a dispersion of Co-*p*ABA capsids in toluene (15 mg mL^{-1}) over a petri dish containing water. The evaporation of the solvent at the air–water interface leads to self-assembled films (Figure 4e–g; Supporting Information, Figure S23). The Co-*p*ABA capsids fuse to bulk self-standing material, as stabilized by the *p*ABA-mediated hydrogen bonds. The capsids do not collapse during drying, as shown in Figure 4f where a fracture surface allows to resolve an individual capsid. Using the Co-*p*ABA with 1.0:0.40 mol ratio, the density of the film is 1.90 g cm^{-3}, which is 20% of the bulk cobalt matter, where the wall thickness of the porous framework (that is, capsid) is about 25–30 nm.

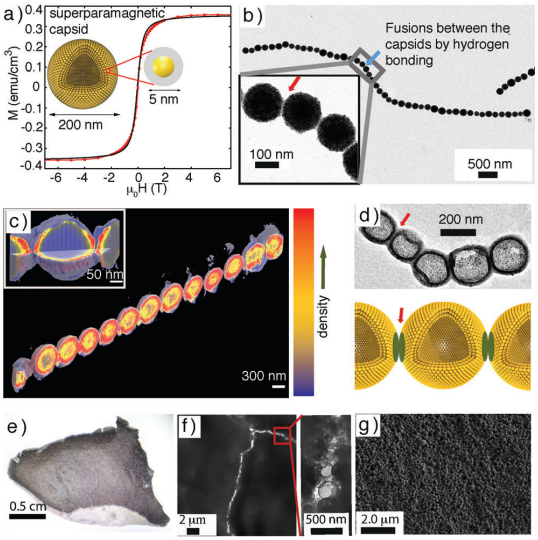

Figure 4. Higher-order capsid structures by directed self-assembly. a) Magnetization curve of Co-*p*ABA capsids showing superparamagnetism. b) Supracolloidal 1D chain of 47 capsids. c) ET reconstruction of a capsid chain. d) Capsid chain upon solvent exchange to acetone. The capsid chains are formed by exposing to magnetic field, and stabilized by hydrogen bonds. e) A freestanding film casted from Co-*p*ABA capsids by interfacial self-assembly. f) The dried Co-*p*ABA capsids do not collapse, as revealed using TEM on a fractured surface, allowing to resolve an individual capsid. g) SEM image of the dried film surface showing the packed Co-*p*ABA capsids.

In summary, we foresee that synthetic capsid-like colloidally self-assembled materials based on nanoparticles as driven by ligand-driven hydrogen bonds pave the way towards modular functional hollow assembies that are relevant to reversible confinement and encapsulation.

Acknowledgements

Funding from Academy of Finland for academy professorship (O.I. and H.H.), CoE in Molecular Engineering of Biosynthetic Hybrid Materials (HYBER, 2014–2019), ERC Advanced Grant MIMEFUN (2012–2017) and DynaSLIPS (J.V.I.T., project number 626954) are acknowledged. This work made use of the CSC-IT centre (Espoo) computational

facilities and Aalto University Nanomicroscopy Center (Aalto-NMC) premises.

Conflict of interest

The authors declare no conflict of interest.

Keywords: capsids · colloidal self-assembly · electron tomography · hydrogen bonding · magnetic nanoparticles

How to cite: *Angew. Chem. Int. Ed.* **2017**, *56*, 6473 – 6477
Angew. Chem. **2017**, *129*, 6573 – 6577

[1] F. Li, D. P. Josephson, A. Stein, *Angew. Chem. Int. Ed.* **2011**, *50*, 360 – 388; *Angew. Chem.* **2011**, *123*, 378 – 409.
[2] a) V. N. Manoharan, *Science* **2015**, *349*, 1253751; b) M. N. O'Brien, M. R. Jones, C. A. Mirkin, *Proc. Natl. Acad. Sci. USA* **2016**, *113*, 11717 – 11725.
[3] a) C. A. Mirkin, R. L. Letsinger, R. C. Mucic, J. J. Storhoff, *Nature* **1996**, *382*, 607 – 609; b) A. P. Alivisatos, K. P. Johnsson, X. Peng, T. E. Wilson, C. J. Loweth, M. P. Bruchez, Jr., P. G. Schultz, *Nature* **1996**, *382*, 609 – 611.
[4] A. K. Boal, F. Ilhan, J. E. DeRouchey, T. Thurn-Albrecht, T. P. Russell, V. M. Rotello, *Nature* **2000**, *404*, 746 – 748.
[5] L. Manna, D. J. Milliron, A. Meisel, E. C. Scher, A. P. Alivisatos, *Nat. Mater.* **2003**, *2*, 382 – 385.
[6] S. Deka, S. Miszta, D. Dorfs, A. Genovese, G. Bertoni, L. Manna, *Nano Lett.* **2010**, *10*, 3770 – 3776.
[7] K. Liu, N. N. Zhao, E. Kumacheva, *Chem. Soc. Rev.* **2011**, *40*, 656 – 671.
[8] a) T. Liu, E. Diemann, H. Li, A. W. Dress, A. Müller, *Nature* **2003**, *426*, 59 – 62; b) Y. Xia, T. D. Nguyen, M. Yang, B. Lee, A. Santos, P. Podsiadlo, Z. Tang, S. C. Glotzer, N. A. Kotov, *Nat. Nanotechnol.* **2011**, *6*, 580 – 587.
[9] a) M. M. Maye, I. S. Lim, J. Luo, Z. Rab, D. Rabinovich, T. Liu, C.-J. Zhong, *J. Am. Chem. Soc.* **2005**, *127*, 1519 – 1529; b) Y. Wang, O. Zeiri, M. Raula, B. L. Ouay, F. Stellacci, I. A. Weinstock, *Nat. Nanotechnol.* **2016**, *12*, 170 – 176.
[10] a) J. J. Benkoski, S. E. Bowles, B. D. Korth, R. L. Jones, J. F. Douglas, A, Karim, J. Pyun, *J. Am. Chem. Soc.* **2007**, *129*, 6291 – 6297; b) J. Pyun, *Angew. Chem. Int. Ed.* **2012**, *51*, 12408 – 12409; *Angew. Chem.* **2012**, *124*, 12576 – 12578.
[11] Z. L. Zhang, Z. Y. Tang, N. A. Kotov, S. C. Glotzer, *Nano Lett.* **2007**, *7*, 1670.
[12] a) C. R. van den Brom, P. Rudolf, T. T. M. Palstra, B. Hessen, *Chem. Commun.* **2007**, 4922; b) C. R. van den Brom, I. Arfaoui, T. Cren, B. Hessen, T. T. M. Palstra, J. T. M. D. Hosson, P. Rudolf, *Adv. Funct. Mater.* **2007**, *17*, 2045 – 2052.
[13] F. Li, W. C. Yoo, M. B. Beernink, A. Stein, *J. Am. Chem. Soc.* **2009**, *131*, 18548 – 18555.
[14] M. A. Kostiainen, P. Hiekkataipale, A. Laiho, V. Lemieux, J. Seitsonen, J. Ruokolainen, P. Ceci, *Nat. Nanotechnol.* **2013**, *8*, 52 – 56.
[15] a) A. H. Gröschel, A. Walther, T. I. Löbling, F. H. Schacher, H. Schmalz, A. H. E. Müller, *Nature* **2013**, *503*, 247 – 251; b) T. I. Löbling, O. Borisov, J. S. Haataja, O. Ikkala, A. H. Gröschel, A. H. E. Müller, *Nat. Commun.* **2016**, *7*, 12097.
[16] G. Singh, H. Chan, A. Baskin, E. Gelman, N. Repnin, P. Král, R. Klajn, *Science* **2014**, *345*, 1149 – 1153.
[17] B. Yoon, W. D. Luedtke, R. N. Barnett, J. Gao, A. Desireddy, B. E. Conn, T. Bigioni, U. Landman, *Nat. Mater.* **2014**, *13*, 807 – 811.
[18] E. Auyeung, T. I. N. G. Li, A. J. Senesi, A. L. Schmucker, B. C. Pals, M. O. de la Cruz, C. A. Mirkin, *Nature* **2014**, *505*, 73 – 77.
[19] a) J. Majoinen, J. Hassinen, J. S. Haataja, H. T. Rekola, E. Kontturi, M. A. Kostiainen, R. H. A. Ras, P. Törmä, O. Ikkala, *Adv. Mater.* **2016**, *28*, 5262 – 5267; b) J.-M. Malho, M. Morits, T. I. Löbling, Nonappa, J. Majoinen, F. H. Schacher, O. Ikkala, A. H. Gröschel, *ACS Macro Lett.* **2016**, *5*, 1185 – 1190; c) T. T. T. Myllymäki, Nonappa, H. Yang, V. Liljeström, M. A. Kostiainen, J.-M. Malho, X. X. Zhu, O. Ikkala, *Soft Matter* **2016**, *12*, 7159 – 7165.
[20] Nonappa, T. Lahtinen, J. S. Haataja, T.-R. Tero, H. Häkkinen, O. Ikkala, *Angew. Chem. Int. Ed.* **2016**, *55*, 16035 – 16038; *Angew. Chem.* **2016**, *128*, 16269 – 16272.
[21] a) D. J. Kushner, *Bacteriol. Rev.* **1966**, *32*, 302 – 345; b) S. Katen, A. Zlotnick, *Methods Enzymol.* **2009**, *455*, 395 – 417; c) A. J. Olson, Y. H. E. Hu, E. Keinan, *Proc. Natl. Acad. Sci. USA* **2007**, *104*, 20731 – 20736.
[22] a) F. Caruso, R. A. Caruso, H. Möhwald, *Science* **1998**, *282*, 1111 – 1114; b) J. Guo, B. L. Tardy, A. J. Christofferson, Y. Dai, J. J. Richardson, W. Zhu, M. Hu, Y. Ju, J. Gui, R. R. Dagastine, I. Yarovsky, F. Caruso, *Nat. Nanotechnol.* **2016**, *11*, 1105 – 1111; c) H. Kim, E. Pippel, U. Gösele, M. Knez, *Langmuir* **2009**, *25*, 13284 – 13289; d) Y. Xia, Z. Tang, *Adv. Funct. Mater.* **2012**, *22*, 2585 – 2593.
[23] M. Yang, H. Chan, G. Zhao, J. H. Bahng, P. Zhang, P. Král, N. A. Kotov, *Nat. Chem.* **2017**, *9*, 287 – 294.
[24] a) V. F. Puntes, K. M. Krishnan, A. P. Alivisatos, *Science* **2001**, *291*, 2115 – 2117; b) J. V. I. Timonen, E. T. Seppälä, O. Ikkala, R. A. Ras, *Angew. Chem. Int. Ed.* **2011**, *50*, 2080 – 2084; *Angew. Chem.* **2011**, *123*, 2128 – 2132.
[25] A. D. Dinsmore, M. F. Hsu, M. G. Nikolaides, M. Marquez, A. R. Bausch, D. A. Weitz, *Science* **2002**, *298*, 1006 – 1009.
[26] H. H. Pham, C. D. Taylor, N. J. Henson, *J. Phys. Chem. B* **2013**, *117*, 868 – 876.
[27] a) L. Guan, L. Rizzello, G. Battaglia, *Nanomedicine* **2015**, *10*, 2757 – 2780; b) V. Percec, et al., *Science* **2010**, *328*, 1009 – 1014; c) M. T. Lombardo, L. D. Pozzo, *Langmuir* **2015**, *31*, 1344 – 1352; d) T. Bian, L. Shang, H. Yu, M. T. Perez, L.-Z. Wu, C.-H. Tung, Z. Nie, Z. Tang, T. Zhang, *Adv. Mater.* **2014**, *26*, 5613 – 5618.
[28] a) J. Mortensen, L. Hansen, K. Jacobsen, *Phys. Rev. B* **2005**, *71*, 035109; b) J. Enkovaara, et al., *J. Phys. Cond. Mater.* **2010**, *22*, 253202.
[29] P. D. Jadzinsky, G. Calero, C. J. Ackerson, D. A. Bushnell, R. D. Kornberg, *Science* **2007**, *318*, 430 – 433.

Manuscript received: February 1, 2017
Revised manuscript received: March 13, 2017
Version of record online: April 28, 2017

